An Energy Harvesting System with Reconfigurable Piezoelectric Energy Harvester Array for IoT Applications

Zhen Li[1], Zhiyuan Chen[1], Qiping Wan[2], Qin Kuai[2], Junrui Liang[3], Philip K.T. Mok[2], Xiaoyang Zeng[1]
Email: {19112020037, chen_zy, xyzeng}@fudan.edu.cn
[1]State Key Laboratory of ASIC and System, Fudan University, Shanghai, China
[2]The Hong Kong University of Science and Technology, Hong Kong, China
[3]ShanghaiTech University, Shanghai, China

***Abstract*—This work presents the novel integration of a reconfigurable piezoelectric energy harvester array (RPA) with a parallel synchronized switch harvesting on inductor (P-SSHI) rectifier. The proposed design realizes maximum power point tracking (MPPT) by adjusting RPA with changes in vibration amplitude. Compared with the traditional interface systems based on monolithic piezoelectric energy harvester (PEH), this design can operate in a wider range of input voltage, removing the need for a DC-DC converter, essential in the traditional design. This adaptability eliminates the need for extra-passive components and reduces switching loss. RPA can be also configured in series to reduce the inherent capacitance of PEHs, effectively improving the extraction efficiency of P-SSHI rectifier. Simulations of this system show that the efficiency of the RPA/P-SSHI combined system can be kept above 66% within an input voltage range from 0.03V to 4.39V.**

Keywords—Piezoelectric energy harvesting, reconfigurable array, maximum power point tracking, parallel synchronized switch harvesting on inductor, rectifier.

I. INTRODUCTION

With the development of the Internet-of-Things (IoT), more sensor nodes are required to realize a better interaction between people and the surrounding environment. Sensors associated with these applications are usually powered by batteries; however, a 1cm^3 lithium battery can only provide an average power load of 100 μW per year [1]. Power supply has, thus, become the main limiting factor for sensor nodes, and energy acquisition technologies such as harvesting thermal energy, light energy and kinetic energy have all been proposed as solutions to this problem [2]. Piezoelectric energy harvesters (PEHs) are widely used in the field of kinetic energy acquisition due to their high power density, easy scaling, and relatively high output voltage [3]. Previous research on PEH has mainly focused on interface circuit design. The full bridge rectifier (FBR) circuit is a popular interface circuit in commercial power management unit because of its simple and stable characteristics, but the energy extraction efficiency is limited due to the inherent capacitance C_p of PEH. Several methods have been reported to reduce this power loss, such as synchronous electric charge extraction (SECE) [4], parallel-synchronized switch harvesting on inductor (P-SSHI) [1] and parallel-synchronized switch harvesting on capacitors (P-SSHC) [5]. P-SSHI is especially promising as it reuses the charge on C_p to reverse the voltage polarity, achieving high power efficiency [3] [5] while also requiring fewer external components than P-SSHC. Development of PEH interface systems still face some challenges: firstly, when the vibration amplitude is low, the open circuit voltage of PEH is only several tens of mV as rectifier is unable to extract power from PEH at such a low amplitude. This leads to a narrow input voltage range and the PEH system's low time availability. Secondly, the output voltage of the rectifier needs to be converted to the required voltage by a DC-DC converter; the intrinsic loss from the converter therefore leads to the reduction of the total available power of the load.

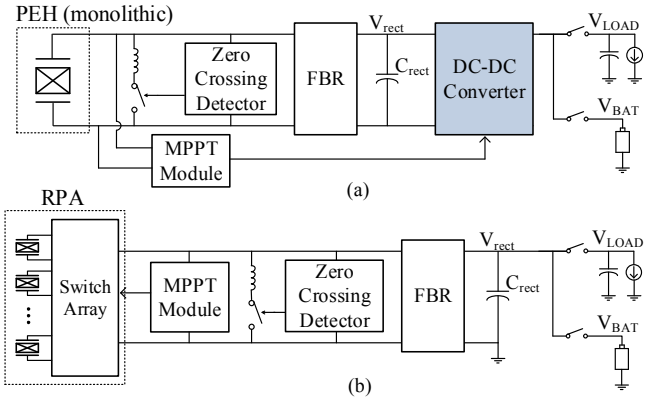

Fig. 1. (a) Conventional PEH system, (b) PEH system based on RPA and the P-SSHI rectifier

One possible solution to extending the input range and improving the efficiency of power conversion is the use of a reconfigurable power source array to provide energy to the system, which has been achieved in light energy harvesting and thermoelectric energy harvesting systems [6, 7]. In the field of piezoelectric energy harvesting, a 4×1 PEH array was proposed in [5] to reduce the flipping capacitance of P-SSHC. However, only two configurations are implemented in this array, therefore limiting both the input range and power conversion efficiency. In this work, we present a novel PEH interface system based on RPA, including a newly-developed P-SSHI rectifier. The proposed circuit omits a DC-DC converter, saving the cost of extra-passive components and reducing switching loss. We also propose to realize maximum power point tracking (MPPT) by adjusting the combination of RPA, obtaining a wider input voltage range. Furthermore, we demonstrate that the inherent capacitance of PEH can be reduced by connecting RPA units in series, improving the energy harvesting efficiency of the P-SSHI rectifier. The rest of this paper is organized as follows: Section II discusses the detailed operation principle and theoretical analysis of the system. Section III outlines the circuit architecture of the proposed PEH interface with a detailed discussion of each building block. Section IV summarizes the results of simulations. Finally, Section V discusses the conclusions of these research efforts.

978-1-7281-3320-1/20/$31.00 ©2020 IEEE

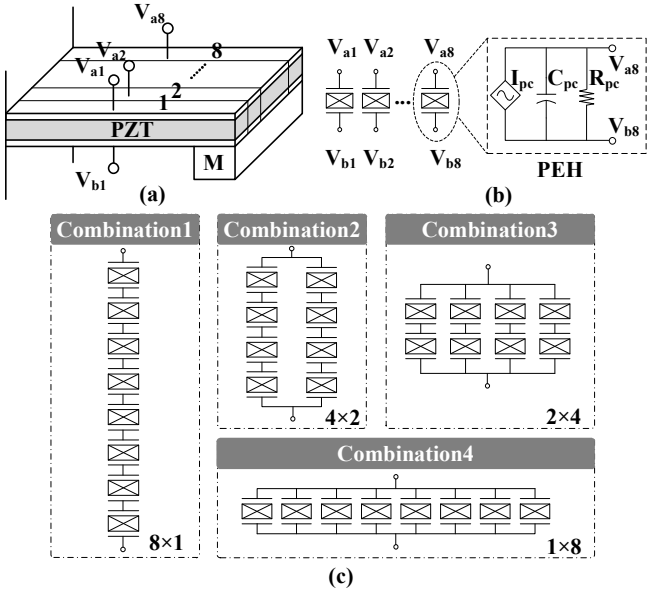

Fig. 2. Representation of RPA: (a) physical structure, (b) equivalent electrical model and symbol, (c) proposed configurations.

II. THEORETICAL ANALYSIS OF RPA

A. The operating mechanism of RPA

Fig. 1 compares the proposed RPA system with a conventional monolithic PEH system. As shown in Fig. 1(a), a conventional PEH generates electrical power from mechanical vibration, the open circuit voltage related to the electrostatic force. In energy harvesting systems, MPPT, usually realized by impedance matching, is necessary to extract the maximum available power generated by PEHs as the input power varies according to the surrounding environment. In practice, conventional circuits achieve MPPT by manipulating the equivalent input impedance of DC-DC power converters, such as switch mode power converters (SMPC) or switched capacitor power converters (SCPC), to convert the input voltage to the required output voltage. However, both types of power converter suffer from drawbacks, in particular the need for the extra passive components and their intrinsic power loss.

Following the trend towards miniaturization and with the availability of high-power density, miniature PEH arrays can now be fabricated via the MEMS process [5]. The output voltage of PEH can also now be tuned by using a reconfigurable PEH array where the equivalent open circuit voltage of PEH array system is adjusted by changing the series parallel combination inside the array. Combining these two advances into one unconventional structure for piezoelectric energy harvesting is proposed in Fig. 1 (b). In this novel system, MPPT is realized not through internal resistance of PEH by adjusting the equivalent input impedance of the DC-DC converters but instead optimize the series of parallel combination of PEHs by re-configuring the PEH array to best suit different environments. For example, when vibration is minimal, the PEHs can be connected in series to increase the voltage of the open circuit. However, when force of vibration rises, the PEH array reconfigures in parallel, ensuring the system operates at near the maximum power point. As discussed in Section IV, the performance of RPA with P-SSHI was verified and compared to RPA with FBR as reference. When the zero-crossing detector is powered on, the system can be regarded as RPA followed by a P-SSHI rectifier (RPA-SSHI mode). Otherwise, the system can be regarded as RPA followed by FBR (RPA-FBR mode).

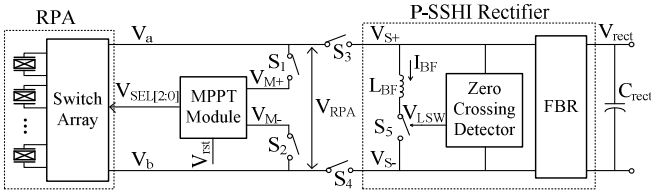

Fig. 3. Block diagram of the proposed system

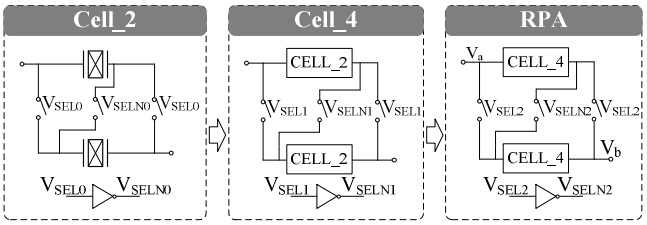

Combination	8×1	4×2	2×4	1×8
$V_{SEL[2:0]}$	000	100	110	111

Fig. 4. Hierarchical structure implementation of the proposed RPA

B. The model and the structure of RPA

The structure of RPA is shown in Fig. 2(a). The entire PEH is divided equally into 8 PEH cells, each cell having its own positive and negative electrodes. As shown in Fig. 2(b), the electrical model of a PEH cell can be represented as a current source I_{pc} in parallel with a capacitor C_{pc} and a resistor R_{pc}. The open circuit voltage amplitude of each PEH cell is V_{pc}. The combinations of RPA are shown in Fig. 2(c). The eight PEH cells form the proposed RPA, which switches among the four combinations according to the amplitude of vibration. When the combination of RPAs is M rows and N columns ($M\times N$=8), the equivalent electrical model of RPA can be represented as a current source I_{RPA} in parallel with a capacitor C_{RPA} and a resistor R_{RPA}, where $I_{RPA}=8\times I_{pc}/M$, $C_{RPA}=8\times C_{pc}/M^2$, $R_{RPA}= M^2\times R_{pc}/8$. The open circuit voltage amplitude of the array can be represented as $V_{RPA}=M\times V_{pc}$. Note that although there are many other combinations for the 8-node array, they cannot meet the maximum power point at the same time with a specific V_{pc}. As such, if the number of PEH cells in each row or column differ from one another, the actual output voltage and the optimal output voltage of each PEH cell will be deviated, resulting in a loss of efficiency in energy conversion. Therefore, only four combinations are proposed in this 8-node system.

C. Power conversion efficiency of the proposed system

To configure RPA properly under different excitation amplitudes, it is necessary to analyze the power conversion efficiency of the system under different combinations of RPA. Comparing the results of this analysis on both the conventional and our new novel system show that the energy harvesting efficiency of an RPA system together with the P-SSHI rectifier can be improved by connecting PEHs in series, reducing of the inherent capacitance of RPA. As the energy harvesting efficiency of FBR and the P-SSHI rectifiers for piezoelectric energy harvesting haven been thoroughly studied [1], we obtain the similar formula for RPA by applying I_{RAP}, C_{RPA} and V_{RAP} (as discussed in Section II-B) to the equations presented in [1]. For simplicity, we assume that the proposed interface is loaded with very large capacitor C_{rect} so that V_{rect} is constant. We

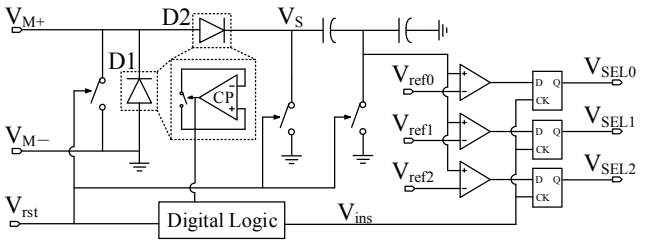

Fig. 5. Structure of MPPT module

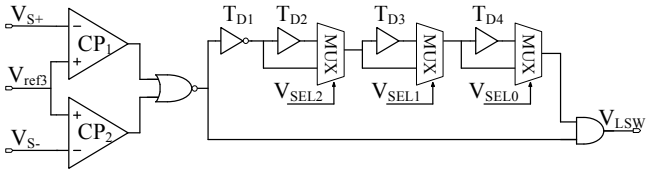

Fig. 6. Structure of proposed RPA based zero-crossing detector

also assume the diodes of FBR are ideal. In the RPA-FBR mode, the power conversion efficiency can be calculated as

$$\eta_{\text{RPA-FBR}} = \frac{4 \cdot \omega_p^2 \cdot C_{\text{pc}}^2 \cdot V_{\text{rect}} \cdot (M \cdot V_{\text{pc}} - V_{\text{rect}})}{M^2 \cdot I_{\text{pc}}^2} \tag{1}$$

Similarly, in the RPA-SSHI mode, the power conversion efficiency can be derived as

$$\eta_{\text{RPA-SSHI}} = \frac{\omega_p^2 \cdot C_{\text{pc}}^2 \cdot V_{\text{rect}} \cdot (2 \cdot M \cdot V_{\text{pc}} - V_{\text{rect}} \cdot \eta_F) \cdot \eta_F}{M^2 \cdot I_{\text{pc}}^2} \tag{2}$$

the factor η_{F} in (2) is the voltage loss ratio, which can be derived as

$$\eta_{\text{F}} = 1 - e^{-\frac{\pi}{\sqrt{\frac{M^2 \cdot L_{\text{BF}}}{2 \cdot R_{\text{BF}}^2 \cdot C_{\text{pc}}} - 1}}} \tag{3}$$

wherein L_{BF} is the bias-flip inductor in the P-SSHI rectifier and R_{BF} is the parasitic resistance of the inductor. The maximum output power increasing rate (MOPIR) in the RPA-SSHI mode can be derived as

$$\text{MOPIR}_{\text{RPA-SSHI}} = \frac{P_{\text{RPA-SSHI,max}}}{P_{\text{RPA-FBR,max}}} = \frac{2}{\eta_{\text{F}}} \tag{4}$$

It can be seen from (3) that η_{F} decreases as the number of rows (M) increases, and thereby $\text{MOPIR}_{\text{RPA-SSHI}}$ increases according to (4), which is also consistent with the simulation results.

III. Implementation of the Proposed System

The structure of the proposed PEH interface circuit system based on an 8-node RPA is shown in Fig. 3. The system is composed mainly of three parts: RPA, the MPPT module, and the P-SSHI rectifier. The system configures the RPA to adjust the open circuit voltage of RPA to implement MPPT, thus avoiding the use of DC converters. The system has two operating modes: the power mode and the MPPT mode. In the power mode, S_1 and S_2 are in the off state, while S_3 and S_4 are in the on state. RPA converts the external vibration into an AC voltage, which is then converted to a DC voltage by the P-SSHI rectifier to supply the load. In the MPPT mode, S_1 and S_2 are in the on state, while S_3 and S_4 are in the off state. RPA is configured to Combination 4,

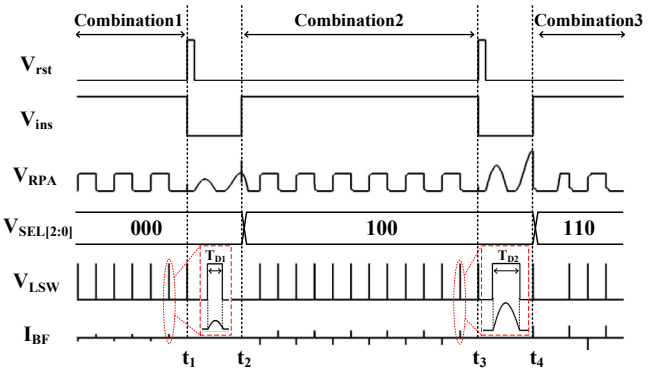

Fig. 7. Simulated waveform of the system control signals

where $V_{\text{RPA}} = V_{\text{pc}}$. The MPPT module detects the peak value of V_{RPA} and, according to the peak value, outputs the $V_{\text{SEL[2:0]}}$ to reconfigure RPA, allowing the system to return to the maximum power point. Detailed circuit diagrams and operations for all the blocks are presented in this section.

A. Reconfigurable PEH Array

Given all the switches in this system are power switches, which cannot be made excessively small, the total area cost is unacceptable when the switch array of RPA is large. Therefore, a hierarchical structure similar to [8] is adopted for RPA implementation, as shown in Fig. 4. A Cell_2 unit includes two PEH cells, three power switches, and one inverter. When the control signal V_{SEL0} is high, the two PEH cells are connected in parallel; otherwise, the PEH cells are connected in series. Similarly, two Cell_2 units form a Cell_4 unit, and two Cell_4 units combine to form the proposed RPA. A total of 21 power switches and 7 inverters are used in the 8-node RPA. We can output $V_{\text{SEL[2:0]}}$ according to the table in Fig. 4 to adjust the combination of RPA.

B. MPPT Module

The design of the MPPT module is similar to [9], its structure is shown in Fig. 5. When MPPT is started, V_{rst} generates a high-level pulse signal, making each switch turn on briefly and thus resetting the voltage of each node. D1 and D2 are two active diodes that form a peak-to-peak detector. It takes 2 cycles to ensure that the value of V_S is equal to the peak-to-peak value of V_{RPA}. After V_S is divided by capacitance, the peak voltage of V_{RPA} is compared with three reference levels V_{ref0}, V_{ref1}, and V_{ref2} to output $V_{\text{SEL[2:0]}}$. The digital module is mainly used to detect the pulse of the CP output in D2. V_S is determined to have reached the peak-to-peak value of V_{RPA} when the rising edge of the second pulse is detected. At that point, the output V_{ins} jumps from a low to high level to sample the flip-flop and thus ends MPPT. V_{ins} is also an indicator of the system's operating mode: when V_{ins}=1, the system is in power mode. However, when V_{ins}=0, the system is in the MPPT mode.

C. P-SSHI rectifier with proposed RPA based zero-crossing detector

The output AC voltage is converted to the required DC voltage by a P-SSHI rectifier. The P-SSHI rectifier includes a FBR, a proposed RPA-based zero-crossing detector, and a flip-in inductor. In this design, the FBR consists of four ideal diodes. The structure of zero-crossing detector is shown in Fig. 6 and is used to turn on S_5 at the time of I_{RPA}=0. When I_{RPA} crosses zero, the diodes of the FBR are moments from turning off. At this instance, one of V_a and V_b (in Fig. 3) is

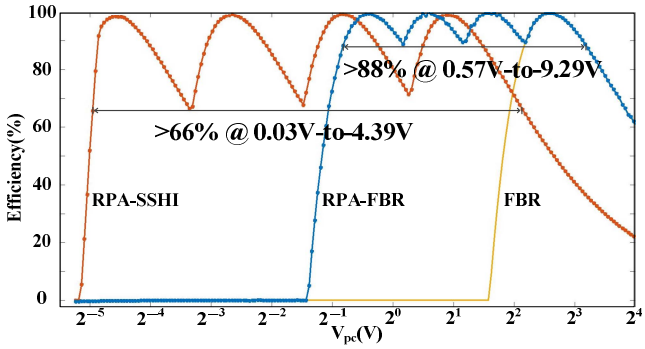

Fig. 8. Power conversion efficiency of FBR, RPA-FBR and the proposed RPA-SSHI

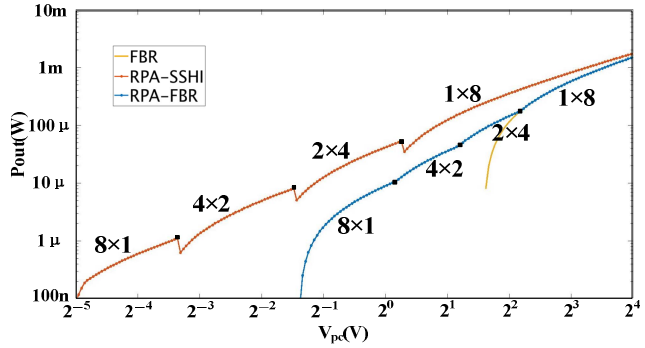

Fig. 9. Output power of FBR, RPA-FBR and the proposed RPA-SSHI

beginning to increase from 0. Hence, CP1 and CP2 are employed to compare V_{S+} and V_{S-} with a reference voltage V_{ref3}=0 to detect this moment. At the moment I_{RPA} crosses 0, the output of CP1 and CP2 is processed by digital units to generate a pulse signal V_{LSW}. S_5 is then turned on by V_{LSW} to close RLC loop to flip V_{RPA}. The pulse width of V_{LSW} can be derived as

$$T_{LSW} = \pi \cdot \sqrt{L_{BF} \cdot C_{RPA}} \qquad (5)$$

Since the L_{BF} size does not change and the value of C_{RPA} varies with the array configuration, T_{LSW} is different under different array combinations. Therefore, the proposed zero-crossing detector adds three delay control units to the traditional circuit. Each delay unit consists of one MUX and one delay unit. When the MUX control terminal is high, the delay unit is connected. The three delay units are controlled by $V_{SEL[2:0]}$ to provide different conduction time to the inductor (L_{BF}) for each RPA combination.

IV. Simulation Results

The settings of the simulation parameters is consistent with the measurement parameters as in [1] (i.e. C_{pc}=6nF, R_{pc}=1.2MΩ, f_p=200Hz, L_{BF}=100µH, R_{BF}=26Ω). V_{rect} is connected to a 3V voltage source. The simulated waveform of the system control signals at the MPPT transition time is shown in the Fig. 7. At the beginning, $V_{SEL[2:0]}$=000, RPA is in Combination 1, and the system works in power mode. A change in V_{pc} at time t_1 causes the system to deviate from the MPP operating point. V_{rst} then generates a high-level pulse to start the MPPT module, while V_{ins} changes from 1 to 0, the system entering MPPT mode. As can be seen from the waveform of V_{RPA}, since the rising edge position of V_{rst} is not within the period of V_{M+}<= V_{M-}, it takes two cycles for the MPPT module to extract the peak-to-peak voltage V_S of V_{RPA}. After that point, V_{SEL} changes from 000 to 100 according to the value of V_S, the RPA changes to

TABLE I.
Summary of RPA-SSHI performance at different combinations

Combination	8×1	4×2	2×4	1×8
C_{RPA}(F)	0.75n	3n	12n	48n
T_{LSW}(S)	0.86µ	1.74µ	3.52µ	7.29µ
η_F	0.110	0.207	0.372	0.615
$MOPIR_{RPA-SSHI}$	4.8x	4.0x	3.2x	2.4x

Combination 2, and V_{ins} changes from low to high level, and the system returns to the power mode. I_{BL} is the current flowing into the L_{BF} during the turn-on of S_5 in Fig. 3. As shown in Fig. 7, the value of T_{LSW} is related to the combination of RPA.

Fig. 8 shows the power conversion efficiency with respect to the input voltage of the RPA-FBR and the RPA-SSHI modes, respectively. The system adjusts the combination of RPAs according to V_{pc} to achieve high efficiency in energy conversion over a wide excitation range. In the RPA-FBR mode, $\eta_{RPA-FBR}$ can maintain an energy efficiency of more than 88% in the range of 0.57V< V_{pc} <9.29V. In the RPA-SSHI mode, $\eta_{RPA-SSHI}$ can maintain an energy efficiency of more than 66% in the range of 0.03V< V_{pc} <4.39V. The control loss of RPA is less than 1%, much smaller than that of DC-DC power converters, as the low frequency operation of the proposed system eliminates the tradeoff between the conduction loss and the switching loss of the DC-DC power converters. Fig. 9 shows the output power with respect to input voltage in FBR, the RPA-FBR and the RPA-SSHI modes, respectively. The output power of P-SSHI with monolithic PEH is equivalent to the 1×8 combination of RPA-FBR. The proposed RPA-SSHI can extend the input power range compared to the monolithic PEH and provide more power than RPA-FBR and FBR. When V_p = 1V, the traditional FBR interface circuit cannot deliver power to the load as the input voltage amplitude is too low. However, under this condition, RPA-FBR and RPA-SSHI can output 9.2µW and 17µW, respectively. Table I lists the impact of RPA combinations on system performance parameters in the RPA-SSHI mode. When RPA is configured in Combination 1, the highest MOPIR the system can reach is 4.8x.

V. Conclusion

This work introduces the design of a PEH system based on an 8-node RPA. This system realizes MPPT by changing the combination of RPA under different excitation amplitudes, avoiding the use of DC-DC converters and the resulting loss of power. The scheme also extends the input voltage range of the system and improves the energy conversion efficiency of the P-SSHI rectifier by configuring RPA in series.

Acknowledgment

This work was supported by the National Natural Science Foundation of China under Grant 61525401, the Program of Shanghai Academic/Technology Research Leader under Grant 16XD1400300, the Major Scientific and Technological Innovation Projects of Shanghai Education Commission under Grant 2017-01-07-00-07-E00026, the National Key Research and Development Program of China (No. 2018YFB2202400, No. 2018YFB2202404).

REFERENCES

[1] Y. K. Ramadass and A. P. Chandrakasan, "An Efficient Piezoelectric Energy Harvesting Interface Circuit Using a Bias-Flip Rectifier and Shared Inductor," *IEEE Journal of Solid-State Circuits*, vol. 45, no. 1, pp. 189-204, Jan. 2010.

[2] Q. Kuai, Q. Wan and P. K. T. Mok, "An Auto-Polarity Thermoelectric Energy Harvesting Interface Based on a Boost/Buck-Boost Converter," *IEEE International Symposium on Circuits and Systems*, pp. 1-4, May. 2019.

[3] D. A. Sanchez, J. Leicht, F. Hagedorn, E. Jodka, E. Fazel and Y. Manoli, "A Parallel-P-SSHI Rectifier for Piezoelectric Energy Harvesting of Periodic and Shock Excitations," *IEEE Journal of Solid-State Circuits*, vol. 51, no. 12, pp. 2867-2879, Dec. 2016.

[4] T. Hehn et al., "A Fully Autonomous Integrated Interface Circuit for Piezoelectric Harvesters," *IEEE Journal of Solid-State Circuits*, vol. 47, no. 9, pp. 2185-2198, Sept. 2012.

[5] S. Du, Y. Jia, C. Zhao, G. A. J. Amaratunga and A. A. Seshia, "A Fully Integrated Split-Electrode SSHC Rectifier for Piezoelectric Energy Harvesting," *IEEE Journal of Solid-State Circuits*, vol. 54, no. 6, pp. 1733-1743, Jun. 2019.

[6] I. Lee, W. Lim, A. Teran, J. Phillips, D. Sylvester and D. Blaauw, "21.4 A >78%-efficient light harvester over 100-to-100klux with reconfigurable PV-cell network and MPPT circuit," *IEEE International Solid-State Circuits Conference*, pp. 370-371, Feb. 2016.

[7] Q. Wan and P. K. T. Mok, "A 14-nA, Highly Efficient Triple-Output Thermoelectric Energy Harvesting System Based on a Reconfigurable TEG Array," *IEEE Journal of Solid-State Circuits*, vol. 54, no. 6, pp. 1720-1732, June 2019.

[8] Q. Wan, Y. Teh, Y. Gao and P. K. T. Mok, "Analysis and Design of a Thermoelectric Energy Harvesting System With Reconfigurable Array of Thermoelectric Generators for IoT Applications," *IEEE Transactions on Circuits and Systems I: Regular Papers*, vol. 64, no. 9, pp. 2346-2358, Sept. 2017.

[9] Z. Chen, Y. Jiang, M. Law, P. Mak, X. Zeng and R. P. Martins, "27.3 A Piezoelectric Energy-Harvesting Interface Using Split-Phase Flipping-Capacitor Rectifier and Capacitor Reuse Multiple-VCR SC DC-DC Achieving 9.3× Energy-Extraction Improvement," *IEEE International Solid-State Circuits Conference*, pp. 424-426, Feb. 2019.